ARE QSO2 HIDING AMONG EROS?

M. BRUSA*

Dipartimento di Astronomia Università di Bologna &
INAF–Osservatorio Astronomico di Bologna,
via Ranzani, 1
I–40127 Bologna
E-mail: brusa@bo.astro.it

We present the results of a deep (80 ks) XMM-*Newton* survey of the largest sample of near-infrared selected Extremely Red Objects (R-K > 5) available to date ($\sim$ 300 objects[1]). The fraction of individually detected, X–ray emitting EROs is of the order of $\sim$ 3.5%, down to $F_x \gtrsim 4 \times 10^{-15}$ cgs and $Ks < 19.2$. In order to derive the X–ray intrinsic properties of AGN EROs and to place our findings in a broader context, we have also considered all the X-ray detected EROs available in the literature. The X-ray, optical, and near-infrared properties of those X-ray selected EROs with a spectroscopic or photometric redshift nicely match those expected for quasars 2, the high-luminosity, high-redshift obscured AGNs predicted in XRB synthesis models.

1. Introduction

The hard X–ray selection turned out to be very efficient in revealing an AGN population with optical to near–infrared colours redder than those of optically selected QSOs. In this respect, the discovery that a sizable fraction of hard X–ray sources also associated to extremely red objects (EROs) with optical to near–infrared R-K > 5 colour is even more intriguing[2,3,4]. Given the key role played by EROs in the cosmological scenario, hard X–ray observations can help to constrain the fraction of AGN among the ERO population and, at the same time, to provide an exciting opportunity to investigate the link between nuclear activity and galaxy formation[5].

*The results presented at this conference have been obtained in collaboration with Andrea Comastri, Emanuele Daddi, Lucia Pozzetti, Gianni Zamorani, Andrea Cimatti, Cristian Vignali, Fabrizio Fiore, and Marco Mignoli.

1.1. *Fraction of AGN EROS*

In this framework, we have started an extensive program of multiwavelength observations of the largest sample of EROs available to date[1], selected in a contiguous area ($\sim$ 700 arcmin^2) down to a magnitude limit of Ks =19.2. We have obtained a total of $\sim$80 ks observation with XMM–*Newton*; the high–energy throughput of XMM–*Newton*, coupled with the large field of view, are well–suited to assess the fraction of AGN among a statistically significant sample of EROs at relatively bright X–ray fluxes[6].
Among the 257 EROs which fall within the XMM–*Newton* area ($\sim$ 380 arcmin^2) analysed in Brusa et al. (2004), nine are individually detected in the X–rays. The fraction of X–ray detected (i.e. AGN–powered) EROs at Ks=19.2 and $F_{0.5-10keV} \gtrsim 2 \times 10^{-15}$ erg cm^{-2} s^{-1}is therefore $\sim$ 3.5%. Conversely, the fraction of EROs among hard X–ray sources is much higher ($\sim$15%).

1.2. *X–ray to optical properties*

In order to investigate the nature of hard X–ray selected EROs and the link between faint hard X–ray sources and the ERO population, we have collected from the literature a sample of 118 X–ray detected EROs (including 9 in our sample); for 52/118 photometric or spectroscopic redshifts are available (data from Lockman Hole[3], CDFN[7], CDFS[8], literature[4,9,10]). This sample is by no means homogeneous (e.g. the selection criteria for EROs are slightly different, R-K$>$ 5 or I-K$>$ 4 depending on the authors; or the K–coverage is not complete), but could be considered representative of EROs individually detected in the X–rays.
The R–band magnitudes plotted versus the hard X–ray fluxes are reported in Fig. 1 (left panel): about half of the sources show an X–ray–to–optical flux ratio (X/O) larger than 10, shifted up by one order of magnitude from that of BL AGN, confirming independent results from near infrared observations of X–ray sources selected on the basis of their high X/O[11].

2. X–ray Properties of AGN EROs

First results suggested that the AGN population among EROs, although not dominant, shares the same X–ray properties of high luminosity, highly obscured AGN, the so–called quasar 2 (QSO2)[3,12,13].
In order to check whether X-ray absorption is common among these objects, we have quantitatively estimated the intrinsic X–ray column densities for

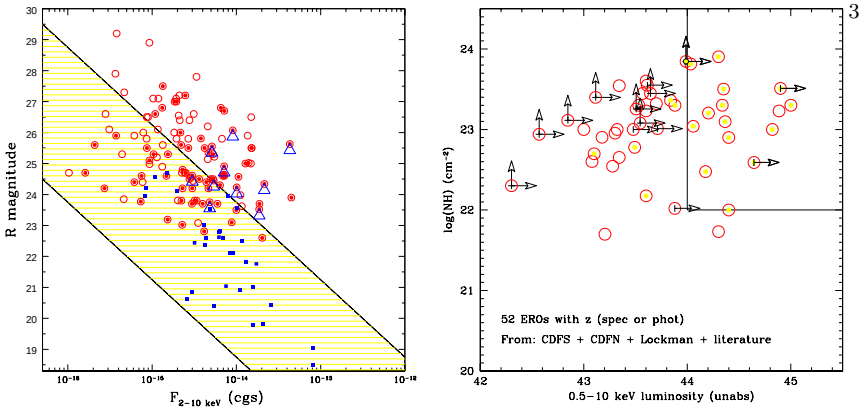

Figure 1. (*left panel*) R–band magnitude vs. hard X–ray flux for EROs, serendipitously detected in hard X–ray surveys. (Triangles = EROs in the "Daddi Field"; Open circles = EROs in the reference sample; filled circles = EROs with redshifts – see text for details). Broad Line AGN detected in the CDFS and CDFN surveys are also reported (small squares). The shaded area represents the region occupied by known AGN (e.g. quasars, Seyferts, emission line galaxies) along the correlation $\log(X/O) = 0 \pm 1$. (*right panel*) Logarithm of the unabsorbed, full band X–ray luminosity versus the logarithm of the absorbing column density (N_H) for all the X–ray detected EROs with spectroscopic or photometric redshifts from the comparison sample (open circles). Filled symbols are EROs with X/O > 10 (see text). The boxy region indicates the locus of QSO2.

the 52 EROs with a reliable spectroscopic or photometric identification. Column densities for the sources detected in the CDFN and CDFS have been obtained by fitting the observed counts with a single power law model plus absorption in the source rest–frame. For the sources in the Lockman Hole and in the "Literature" sample, the best–fit values quoted by the authors have been adopted. In all the cases, X–ray luminosities were estimated from the observed X–ray fluxes and corrected for absorption. The results are reported in the right panel of Fig. 1.

Almost all of the individually detected EROs have intrinsic $N_H > 10^{22}$ cm^{-2}, and they actually *are* heavily obscured AGN. This study confirms previous evidences mainly based on a Hardness Ratio analysis[12] and on few isolated examples[9,4,14], and unambiguously indicates that large columns of cold gas (even $> 10^{23}$ cm^{-2}) are the rule rather than the exception among X–ray bright EROs.

3. EROs and QSO2: a selection criterion

Given the high–redshift of these objects ($z \gtrsim 1$) and the average X–ray flux of the comparison sample ($\sim 4 \times 10^{-15}$ erg cm^{-2} s^{-1}), it is not surprising that the majority of X–ray detected EROs have high X–ray luminosities

($L_X > 10^{43}$ erg s^{-1}). Moreover, according to our analysis, a significant fraction of them have X–ray luminosities exceeding 10^{44} erg s^{-1}, and therefore lie within the quasar regime. The large intrinsic column densities further imply that AGN EROs, selected at the brightest X–ray fluxes, have properties similar to those of QSO2, the high–luminosity, high–redshift Type 2 AGNs predicted by X–Ray Background synthesis models[15,16]. Among the X–ray detected EROs, the higher is the luminosity, the higher is the X–ray to optical flux ratio (filled symbols in right panel of Fig. 1). This confirms that a selection based on X/O > 10 is a powerful tool to detect high–luminosity, highly obscured sources, and it is even stronger when coupled with a previous selection on the extremely red colors.
Given that the search for QSO2 on the basis of detection of narrow optical emission lines is very difficult and is already challenging the capabilities of the largest optical telescopes, the proposed "alternative" method which combines near–infrared and X–ray observations, could provide a powerful tool to uncover luminous, obscured quasars.

Acknowledgments

I kindly acknowledge support by INAOE, Mexico, during the 2003 Guillermo-Haro Workshop where part of this work was performed.

References

1. E. Daddi et al., *A.&A.* **361**, 535 (2000).
2. I. Lehmann et al., in *"X-rays at Sharp Focus Chandra Science Symposium"*, astro–ph/0109172 (2001).
3. V. Mainieri et al., *A.&A.* **393**, 425 (2002).
4. C. Willott et al. *M.N.R.A.S.* **339**, 397 (2003).
5. G.L. Granato et al., *M.N.R.A.S.* **324**, 757 (2001).
6. M. Brusa et al., *A.&A.* , submitted, (2004).
7. A.J. Barger et al., *A.J.* **126**, 632 (2003).
8. G.P. Szokoly et al., *Ap.J.S.S.* , , submitted, astro–ph/0312324 (2004).
9. C.S. Crawford et al., *M.N.R.A.S.* **324**, 427 (2001).
10. M. Brusa et al., *A.&A.* **409**, 65 (2003).
11. M. Mignoli et al., *A.&A.* , in press, astro–ph/0401298 (2004).
12. D.M. Alexander et al., *A.J.* **123**, 1149 (2002).
13. P. Severgnini et al, in *"Multiwavelength Mapping of Galaxy Formation and Evolution"*, astro–ph/0312098 (2004).
14. J.A. Stevens et al., *M.N.R.A.S.* **342**, 249 (2003).
15. A. Comastri et al., *M.N.R.A.S.* **327**, 781 (2001).
16. R. Gilli, M. Salvati and G. Hasinger *A.&A.* **336**, 407 (2001).